

Separation of Styrene and Ethylbenzene on Metal–Organic Frameworks: Analogous Structures with Different Adsorption Mechanisms

Michael Maes,[†] Frederik Vermoortele,[†] Luc Alaerts,[†] Sarah Couck,[‡]
Christine E. A. Kirschhock,[†] Joeri F. M. Denayer,[‡] and Dirk E. De Vos*[†]

Centre for Surface Chemistry and Catalysis, Katholieke Universiteit Leuven, Arenbergpark 23,
B-3001 Leuven, Belgium, and Department of Chemical Engineering, Vrije Universiteit Brussel,
Pleinlaan 2, B-1050 Brussel, Belgium

Received July 12, 2010; E-mail: dirk.devos@biw.kuleuven.be

Abstract: The metal–organic frameworks MIL-47 ($V^{IV}O\{O_2C-C_6H_4-CO_2\}$) and MIL-53(Al) ($Al^{III}(OH)\cdot\{O_2C-C_6H_4-CO_2\}$) are capable of separating ethylbenzene and styrene. Both materials adsorb up to 20–24 wt % of both compounds. Despite the fact that they have identical building schemes, the reason for preferential adsorption of styrene compared to ethylbenzene is very different for the two frameworks. For MIL-47, diffraction experiments reveal that styrene is packed inside the pores in a unique, pairwise fashion, resulting in separation factors as high as 4 in favor of styrene. These separation factors are independent of the total amount of adsorbate offered. This is due to co-adsorption of ethylbenzene in the space left available between the packed styrene pairs. The separation is of a non-enthalpic nature. On MIL-53, the origin of the preferential adsorption of styrene is related to differences in enthalpy of adsorption, which are based on different degrees of framework relaxation. The proposed adsorption mechanisms are in line with the influence of temperature on the separation factors derived from pulse chromatography: separation factors are independent of temperature for MIL-47 but vary with temperature for MIL-53. Finally, MIL-53 is also capable of removing typical impurities like *o*-xylene or toluene from styrene–ethylbenzene mixtures.

1. Introduction

Styrene (**St**) is the most important aromatic monomer produced in industry due to the high reactivity of its vinyl group.¹ Of its production, which currently exceeds 25 million tons per year, more than 80% is used for polymerization into, for example, synthetic rubbers, thermoplastics, or resins. **St** is obtained by dehydrogenation of ethylbenzene (**EB**). As no full conversion is achieved, the product stream still contains a large fraction (20–40%) of unreacted **EB**, which needs to be removed.¹ Because of the high reactivity of the vinyl group of **St** and the fact that the boiling points of **St** (bp 418 K) and **EB** (bp 409 K) are similar, separation by conventional distillation on an industrial scale is not straightforward. Furthermore, small amounts of impurities with similar boiling points, like toluene (bp 393 K) and *o*-xylene (**oX**, bp 418 K), also have to be removed from the **St**–**EB** product stream. These impurities further complicate the conventional distillation.² Expensive technologies like vacuum distillation or extractive distillation have to be applied in the presence of inhibitors like phenylenediamines or dinitrophenols in order to avoid **St** polymerization.^{2–5}

On a smaller scale, another possibility reported in the literature is pervaporation through polyurethane or cross-linked poly(hexamethylenesebacate) membranes.^{6,7}

An interesting alternative is adsorptive separation using porous materials. This technology does not require elevated temperatures; the problem of side reactions can therefore be circumvented, at least if the bed is not reactive itself. Metal–organic frameworks (MOFs) are a family of crystalline microporous materials built from metal ions connected by organic linkers. An enormous variety of pore geometries and chemical functionalities is available in these materials. Furthermore, MOFs have high specific surfaces and pore volumes next to minimal dead volumes, making them suitable candidate materials for adsorptive separation.^{8–14} They have been applied to several relevant liquid-phase separations or purifications, such

[†] Katholieke Universiteit Leuven.

[‡] Vrije Universiteit Brussel.

- (1) *Kirk-Othmer Encyclopedia of Chemical Technology*; John Wiley & Sons, Inc.: New York, 2008; 1040 pp.
- (2) *Ullmann's Encyclopedia of Industrial Chemistry*, 6th ed.; John Wiley & Sons, Inc.: New York, 2006; electronic release.
- (3) Butler, J. R.; Watson, J. M.; Forward, C. H. U.S. Patent 4417085, 1983.
- (4) Berg, L. U.S. Patent 4959128, 1990.

(5) Polimeri Europa, 2009, <http://www.polimerieuropa.it/it/pdf/Styrene.pdf>.

(6) Strazik, W. F.; Perry, E. U.S. Patent 3776970, 1973.

(7) Cao, B.; Hinode, H.; Kajuchi, T. *J. Membr. Sci.* **1999**, *156*, 43–47.

(8) Li, H.; Eddaoudi, M.; O'Keeffe, M.; Yaghi, O. *Nature* **1999**, *402*, 276.

(9) Chui, S.; Lo, S.; Charmant, J.; Orpen, A.; Williams, I. *Science* **1999**, *283*, 1148.

(10) Müller, U.; Schubert, M.; Teich, F.; Pütter, H.; Schierle-Armdt, K.; Pastré, J. *J. Mater. Chem.* **2006**, *16*, 626.

(11) Pan, L.; Olson, D.; Ciemnomolnski, L.; Heddy, R.; Li, J. *Angew. Chem.* **2006**, *118*, 632; *Angew. Chem., Int. Ed.* **2006**, *45*, 616.

(12) Morris, R.; Wheatley, P. *Angew. Chem.* **2008**, *120*, 5044; *Angew. Chem., Int. Ed.* **2008**, *47*, 4966.

(13) Férey, G. *Chem. Soc. Rev.* **2008**, *37*, 196.

(14) Trevin, A.; Cooper, A. *Angew. Chem.* **2010**, *122*, 1575; *Angew. Chem., Int. Ed.* **2010**, *49*, 1533.

as the separation of xylenes or the compounds in the C₅ fraction produced by a steam cracker or removal of heterocyclic aromatic compounds from fuels.^{15–19}

Recently, the MOF HKUST-1 ([Cu₃(BTC)₂]; BTC = 1,3,5-benzenetricarboxylate) has been reported to discriminate between injected aliquots of **EB** and **St** in a liquid-phase tracer chromatographic separation using a MOF column as the adsorbent bed.²⁰ In the present work, the potential of two MOFs with similar structures, MIL-47 and MIL-53(Al), for the separation of **EB**- and **St**-containing feeds is explored.^{21,22} MIL-47 consists of chains of V^{IV} octahedra connected by terephthalate linkers and has diamond-shaped 1D hydrophobic pores with a diameter of approximately 1.1 nm.²¹ The well-known material MIL-53 has a similar structure, built from Al^{III} octahedra. However, there are some differences between the two materials: MIL-53 has hydrophilic pores due to the presence of hydroxyl groups and its structure is known to be flexible, which means that it can dynamically respond to the presence of adsorbates.^{22–26} On both materials an excellent separation of xylenes is obtained, making them interesting candidate materials for the separation of **EB** and **St**.^{15,27} Not only will the separation of **EB** and **St** be examined but also the purification of a simulated process stream containing toluene and **oX** as additional impurities. After assessing the materials' potential for realistic separations, the adsorption mechanisms will be studied on the basis of temperature-dependent pulse chromatographic techniques, vapor-phase adsorption experiments, and Rietveld refinements of the X-ray diffraction (XRD) patterns of the loaded structures.

2. Experimental Section

MIL-47 was synthesized according to the literature by loading a mixture of 1.22 g of VCl₃, 0.32 g of terephthalic acid, and 14 mL of H₂O in a Teflon-lined steel autoclave and placing it in an oven at 473 K for 96 h.²¹ After cooling, the mixture was washed with water and activated by calcination under air for 21.5 h at 573 K.²⁸ MIL-53(Al) was synthesized according to the literature by loading a mixture of 1.88 g of Al(NO₃)₃·9H₂O, 0.41 g of

terephthalic acid, and 3.62 mL of water in a Teflon-lined steel autoclave and placing it in an oven at 493 K for 72 h. After the white powder was washed with water, it was activated by calcination at 603 K for 72 h.²²

Liquid-phase batch adsorption experiments were carried out at 298 K in 1.8 mL glass vials filled with 0.025 g of adsorbent and a binary solution of aromatics in heptane, following a literature procedure.^{15,29} As heptane has no functional group to interact with the host material, it can be considered as a non-interacting solvent, and it will therefore not influence the adsorption capacity or selectivity.^{15,18,27} Uptakes were directly calculated from GC output data. Separation factors α_{ij} were calculated using eq 1:

$$\alpha_{ij} = \left(\frac{q_i}{q_j}\right)\left(\frac{c_j}{c_i}\right) \quad (1)$$

with q_i and q_j the amount (mol g⁻¹) of compounds i and j adsorbed per gram of MOF and c_i and c_j the concentration (mol L⁻¹) of compounds i and j remaining in the external liquid phase.³⁰

Pulse and breakthrough chromatographic experiments were performed following a literature procedure.¹⁵ Columns were handmade by loading approximately 0.6 g of adsorbent into a stainless steel column ($L = 5$ cm, $D = 0.45$ cm) under a nitrogen atmosphere.

For breakthrough experiments, average selectivities were calculated using eq 1. For each compound, the adsorbed amounts q were calculated by integration of the curves using eq 2:

$$q = \int_0^t u(C_{in} - C_{out}) dt \quad (2)$$

with u being the volumetric flow rate of the feed (L min⁻¹) and C_{in} and C_{out} the concentration (mol L⁻¹) of the adsorbate in the liquid feed and eluent, respectively. As the column is fed with an equimolar mixture, the average separation factor α can be written as $\alpha = q_{\text{styrene}}/q_{\text{ethylbenzene}}$. Regeneration of the column is performed by flushing with typically 100 mL of pure solvent at the same temperature and pressure as during adsorption.

Pulse chromatographic experiments were performed at different temperatures by heating a HPLC column filled with both adsorbent and the solvent to the required temperature. The separation factor is then calculated according to eq 3:

$$\alpha_{ij} = \frac{(\mu_i - \mu_{tc})}{(\mu_j - \mu_{tc})} \quad (3)$$

with μ_i the first moment of the second-eluting compound, μ_j the first moment of the first-eluting compound, and μ_{tc} the first moment of 1,3,5-triisopropylbenzene, a tracer compound which is too large to enter the pores and thus is indicative of the dead volume. First moments are calculated using ChemStation software from Agilent.

Details on the calculation of the apparent adsorption enthalpies and the zero-coverage adsorption enthalpies, as well as details on the crystal structure refinements, are given in the Supporting Information.

3. Results and Discussion

Competitive adsorption experiments in static conditions using heptane as a non-interacting solvent show that both MIL-47 and MIL-53 discriminate between **EB** and **St** with high selectivity (Figure 1). On MIL-47, a clear preference for **St** is observed, with a maximal uptake of approximately 20 wt %, which is similar to the value obtained in single-compound

- (15) Alaerts, L.; Kirschhock, C.; Maes, M.; van der Veen, M.; Finsy, V.; Depla, A.; Martens, J.; Baron, G.; Jacobs, P.; Denayer, J.; De Vos, D. *Angew. Chem.* **2007**, *119*, 4371; *Angew. Chem., Int. Ed.* **2007**, *46*, 4372.
- (16) Cychoz, K.; Wong-Foy, A.; Matzger, A. *J. Am. Chem. Soc.* **2009**, *131*, 14538.
- (17) Gu, Z.; Yan, X. *Angew. Chem.* **2010**, *122*, 1519; *Angew. Chem., Int. Ed.* **2010**, *49*, 1477.
- (18) Maes, M.; Alaerts, L.; Vermoortele, F.; Ameloot, R.; Couck, S.; Finsy, V.; Denayer, J.; De Vos, D. *J. Am. Chem. Soc.* **2010**, *132*, 2284.
- (19) Nuzhdin, A.; Kovalenko, K.; Dybtsev, D.; Bukhtiyarova, G. *Mendeleeev Commun.* **2010**, *20*, 57.
- (20) Ahmad, R.; Wong-Foy, A.; Matzger, A. *Langmuir* **2009**, *25*, 11977.
- (21) Barthelet, K.; Marrot, J.; Riou, D.; Férey, G. *Angew. Chem., Int. Ed.* **2001**, *41*, 281.
- (22) Loiseau, T.; Serre, C.; Huguenard, C.; Fink, G.; Taulelle, F.; Henry, M.; Bataille, T.; Férey, G. *Chem.—Eur. J.* **2004**, *10*, 1373.
- (23) Llewellyn, P. L.; Bourrelly, S.; Serre, C.; Filinchuk, Y.; Férey, G. *Angew. Chem.* **2006**, *118*, 7915; *Angew. Chem., Int. Ed.* **2006**, *45*, 7751.
- (24) Liu, Y.; Her, J.; Dailly, A.; Ramirez-Cuesta, A. J.; Neumann, D. A.; Brown, C. M. *J. Am. Chem. Soc.* **2008**, *130*, 11813.
- (25) Trung, T. K.; Trens, P.; Tanchoux, N.; Bourrelly, S.; Llewellyn, P. L.; Loera-Serna, S.; Serre, C.; Loiseau, T.; Fajula, F.; Férey, G. *J. Am. Chem. Soc.* **2008**, *130*, 16926.
- (26) Salles, F.; Jobic, H.; Ghoufi, A.; Llewellyn, P.; Serre, C.; Bourrelly, S.; Férey, G.; Maurin, G. *Angew. Chem.* **2009**, *121*, 8485; *Angew. Chem., Int. Ed.* **2009**, *48*, 8335.
- (27) Alaerts, L.; Maes, M.; Giebel, L.; Jacobs, P.; Martens, J.; Denayer, J.; Kirschhock, C.; De Vos, D. *J. Am. Chem. Soc.* **2008**, *130*, 14170.
- (28) Alaerts, L.; Maes, M.; Jacobs, P.; Denayer, J.; De Vos, D. *Phys. Chem. Chem. Phys.* **2008**, *10*, 2979.

- (29) Alaerts, L.; Maes, M.; van der Veen, M.; Jacobs, P.; De Vos, D. *Phys. Chem. Chem. Phys.* **2009**, *11*, 2903.
- (30) Ruthven, D. M. *Principles of Adsorption and Adsorption Processes*; John Wiley & Sons, Inc.: New York, 1984; 433 pp.

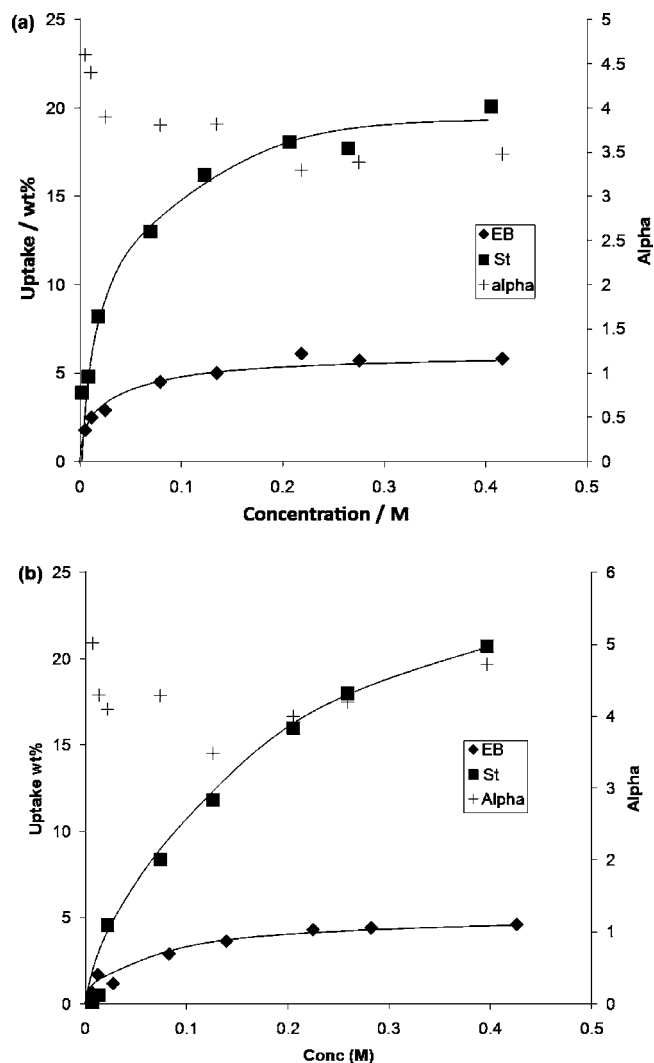


Figure 1. Competitive adsorption on (a) MIL-47 and (b) MIL-53 in batch mode: uptake (wt %) of an equimolar mixture of **EB** and **St** in heptane at room temperature as a function of equilibrium liquid-phase concentration of each compound. Separation factors α are given on the right axis.

Table 1. Uptake Capacities (wt % with Respect to MOF) at 0.45 M of **EB** or **St** Out of Heptane in Single-Compound Batch Experiments on MIL-47 and MIL-53

	MIL-47	MIL-53
St	21	24
EB	16	15

experiments under the same conditions (Table 1). Apparently, the adsorption of **St** is not significantly influenced by the presence of **EB** in the mixture. The uptake of **EB** does not increase beyond 5 wt % in a competitive experiment, while in single-compound mode up to 16 wt % is adsorbed in the studied concentration range (0–0.45 M initial concentrations, Figure 1a, Table 1). The separation factors remain practically constant at a value of 3.6 ± 0.2 . On MIL-53, saturation levels (± 3 wt %) are similar to those obtained on MIL-47 for both competitive and single-compound experiments. As in the case of MIL-47, the separation factors on MIL-53 tend to remain constant at approximately 4.1 ± 0.3 (Figure 1b). The separation factors obtained on both materials exceed the best separation factors reported in the literature under the same conditions, illustrating the MOFs' suitability for this interesting separation.^{6,7} For

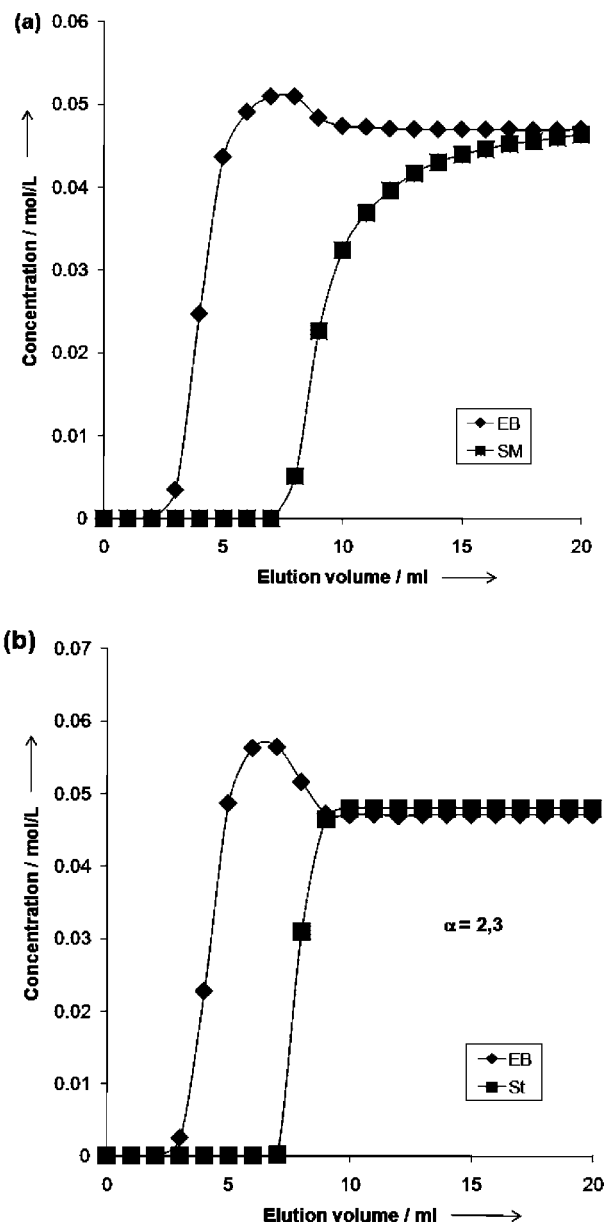


Figure 2. Breakthrough experiments with binary 0.047 M solutions of **EB** and **St** in heptane on (a) MIL-47 and (b) MIL-53 at 298 K. The curves are corrected for the dead volume.

example, a maximal separation factor of 2.5 is obtained using the same mixture composition at room temperature by performing pervaporation on poly(hexamethylenesbacate) membranes.⁷

As both materials are capable of separating **EB** and **St** under static conditions, their potential for a real separation of **EB** and **St** in dynamic conditions was probed by breakthrough experiments using a column filled with MOF crystallites placed in an HPLC apparatus. An equimolar mixture of **EB** and **St** (both 0.047 M) in heptane was forced through this column while the outlet concentrations were monitored. In the case of MIL-47, the breakthrough profile shows an interval of 3 mL during which both compounds are fully retained, whereafter only **EB** is detected at the column outlet during the elution of the next 5 mL (Figure 2a). The outlet concentration of **EB** in this interval is temporarily higher than the inlet value. This so-called roll-up effect is caused by the displacement of **EB** by **St**, showing that **St** competes more successfully for the space in the pores than **EB**. Eventually, at saturation of the column, the outlet

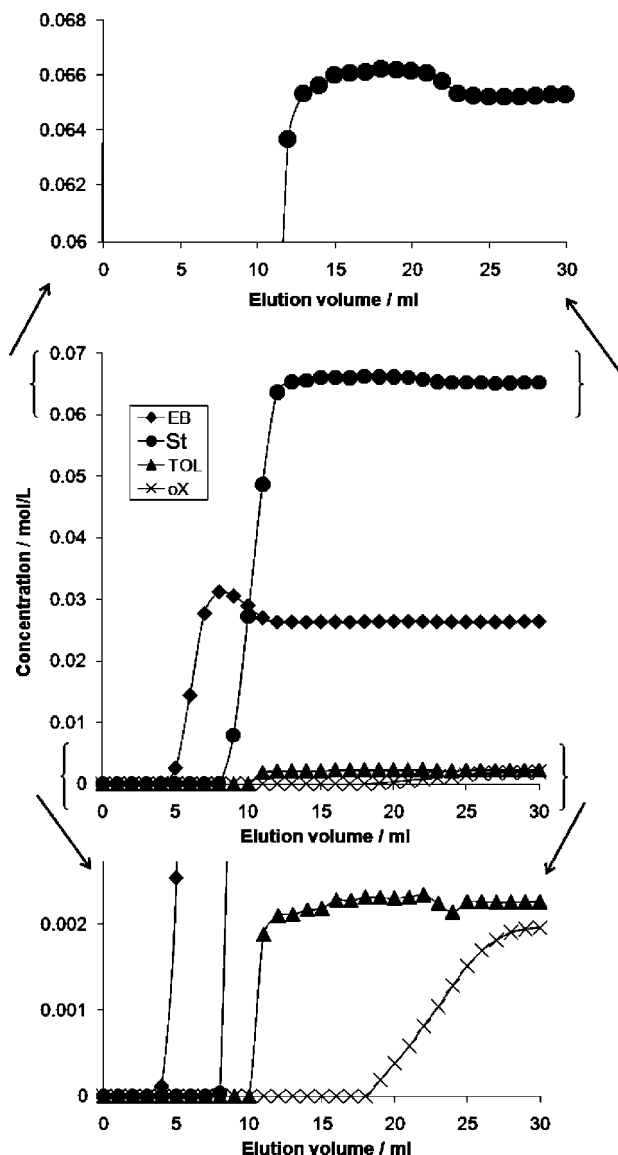


Figure 3. Breakthrough experiment with a mixture of 68 wt % **St**, 28 wt % **EB**, 2 wt % **oX**, and 2 wt % toluene (TOL) with respective concentrations of 0.06, 0.026, 0.002, and 0.002 M in heptane. Experiments were performed at 298 K on MIL-53. The central graph shows the measured breakthrough profile; a detail of the same profile at the lowest concentrations is shown at the bottom. A detail of the curve of **St** at high concentrations is given on top to zoom in on the small roll-up effect, in which **oX** displaces some **St**. The curves are corrected for the dead volume.

concentrations of both compounds are equal to the inlet values. In the case of MIL-53, a similar behavior is observed (Figure 2b). Average separation factors for **St** over **EB** of 2.9 and 2.3 were calculated by integration of the curves for MIL-47 and MIL-53, respectively. Regeneration of both columns was achieved by flushing with 100 mL of pure hydrocarbon solvent (see Supporting Information).

In addition, we performed the combined separation–purification in diluted conditions of a mixture with a more realistic composition that also contains small amounts of typical impurities like toluene and *o*-xylene (**oX**). The literature describes, for instance, a mixture containing 68 wt % **St**, 28 wt % **EB**, 2 wt % **oX**, and 2 wt % toluene.² MIL-53 is known to have a strong preference for *ortho*-substituted alkylaromatics, and as this work has shown that it is also capable of separating **EB** and **St**, this material seems the most suitable candidate to

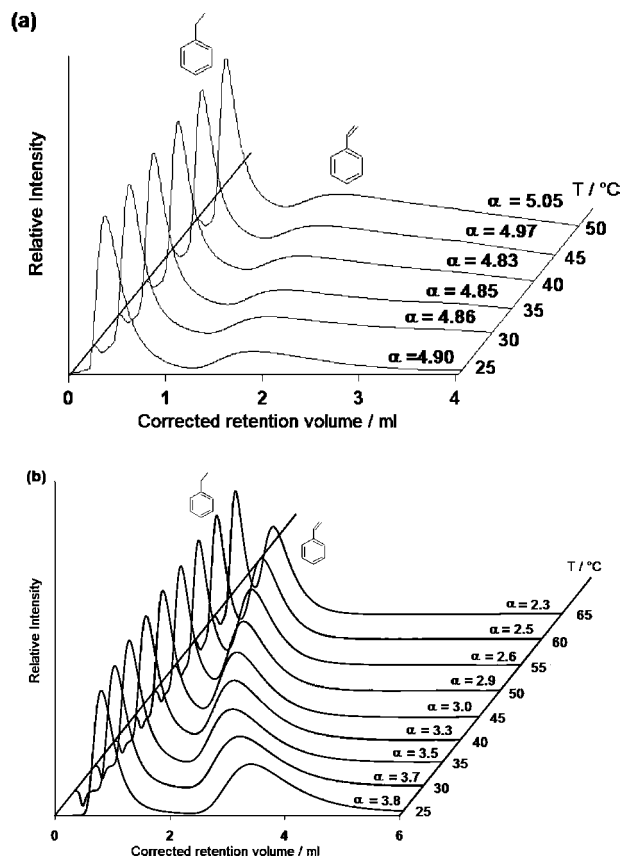


Figure 4. Competitive pulse chromatographic experiments on (a) MIL-47 and (b) MIL-53 at different temperatures. Experiments were performed by injecting 1 μ L of a mixture of **EB** and **St** in heptane. The temperature is shown on the right axis. Separation factors α are given above each chromatogram and represent the preference of **St** over **EB**.

Table 2. Apparent Adsorption Enthalpies ΔH_{app} and Zero Coverage Adsorption Enthalpies ΔH_{zc} (kJ mol^{-1}) of **St** and **EB** on MIL-47 and MIL-53^a

	MIL-47		MIL-53	
	ΔH_{app}	ΔH_{zc}	ΔH_{app}	ΔH_{zc}
St	-9.0 ± 1.4	-57.0 ± 0.4	-24.2 ± 1.2	-59.1 ± 0.7
EB	-10.1 ± 1.8	-57.6 ± 0.5	-13.1 ± 1.4	-48.9 ± 0.5

^a See Supporting Information for calculations and van't Hoff plots.

perform such a combined purification–separation.²⁷ Figure 3 shows the breakthrough profiles on MIL-53 of the quaternary mixture diluted in heptane. As with the binary experiment in Figure 2b, **St** is preferred over **EB**, with a similar average separation factor of 2.2. Toluene and **oX** are retained longer on the column: while **St** elutes at 8 mL, toluene and **oX** elute later, at 11 and 18 mL, respectively. A small roll-up effect is seen in the curve of **St** during the adsorption of **oX**, not only underlining the high resolution of this test but also confirming the strong preference of MIL-53 for *ortho*-disubstituted aromatics. **oX** is able to pack densely in the pores of MIL-53, as has been reported before, due to the interaction of both methyl groups with the hosts' carboxylate groups.²⁷ This allows a more efficient packing of this compound than, for instance, of **St** and **EB**. This results in four molecules of **oX** per unit cell, while **St** and **EB** only reach values of approximately 2 molecules per unit cell (see below).²⁷ Toluene is likely to interact less strongly than **oX**, as it can only interact through one methyl group. It is fair to assume that the location of a toluene molecule is similar to

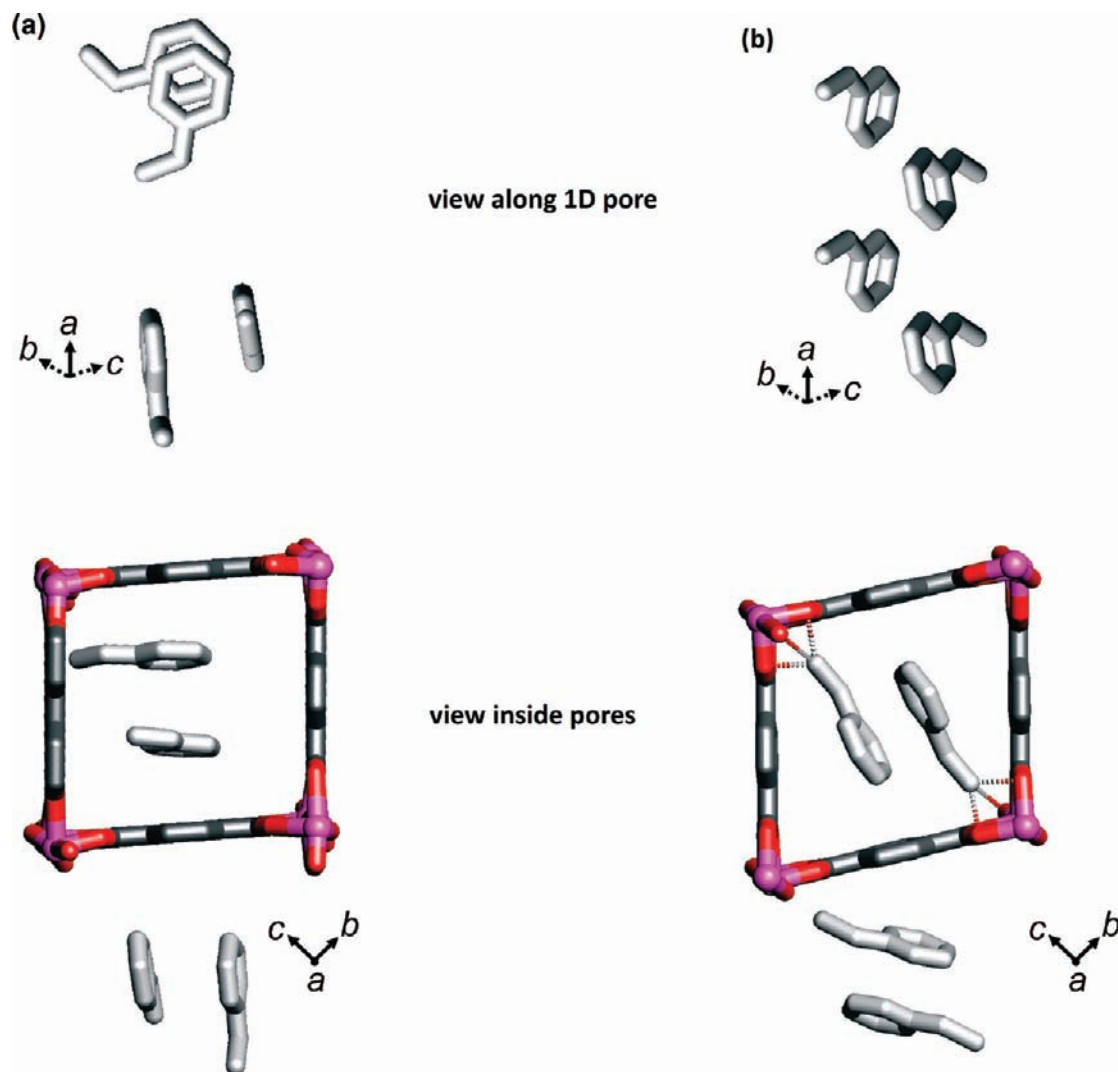


Figure 5. Structure refinement of MIL-47 crystals loaded with (a) **St** and (b) **EB**¹⁵ (dark gray, carbon; red, oxygen; pink, vanadium; hydrogen atoms have been omitted). For **EB**, only half of the positions shown can be occupied simultaneously.

that of *p*-xylene, in which simultaneous interaction of both methyl groups with the pore walls is geometrically impossible.²⁷ Thus, the mechanism of interaction of toluene with the pore wall could be similar to that of other monosubstituted alkylaromatics; however, in practice, it appears that toluene retention under our experimental conditions is higher than that of styrene or ethylbenzene. As an adsorbent bed has only a finite capacity, it is preferred that main components of the feed, in this case **EB** and **St**, elute before the contaminants. As such, the capacity of the material can be optimally used for the removal of these minor impurities; hence, a purified stream of **EB** and **St** can be easily obtained which can be processed for further separation. This makes MIL-53 a more interesting candidate for the combination of separation and purification compared to [Cu₃(BTC)₂], which has been mentioned as an alternative adsorbent in the literature.²⁰ Preliminary batch experiments, combined with results from the literature, revealed that [Cu₃(BTC)₂] shows a different order of preference: while **St** is still preferred over **EB**, **EB** is preferred over both **oX** and toluene (see Supporting Information).¹⁵ **oX** and toluene are thus likely to elute before both **EB** and **St**. This makes [Cu₃(BTC)₂] significantly less suitable for the purification application than the MIL-53 material which is proposed here. Regeneration was again performed by flushing the column with 100 mL of

hydrocarbon solvent. This proves that MIL-53 is capable of selectively removing impurities from the product feed in the first step, followed by separation of **EB** and **St** in the second step.

In order to understand the adsorption mechanism causing the preferential uptake of **St** on both materials, pulse chromatographic experiments were carried out on the same columns at different temperatures. In the case of MIL-47, the peaks of **EB** and **St** are baseline-separated at 298 K, and the separation factor of approximately 5 is independent of temperature in the 298–323 K interval (Figure 4a). This separation factor exceeds the value of 3.9 obtained in the literature on [Cu₃(BTC)₂] by almost 25%.²⁰ The relative retention of the different compounds depends on their adsorption equilibrium constants. In liquid-phase chromatography, the equilibrium constant *K_i* of a given compound *i* reflects the competition between the compound under consideration and the molecules of the mobile phase for adsorption on the surface of the adsorbent.³¹ The negligible dependence of the separation factor on temperature proves that the adsorption enthalpies for **EB** and **St** must be comparable. Apparent adsorption enthalpies for **EB** and **St** on MIL-47 were calculated on the basis of the temperature dependence of the first moment of single-compound chromatographic response curves: both values range between -9.0 ± 1.4 and $-10.1 \pm$

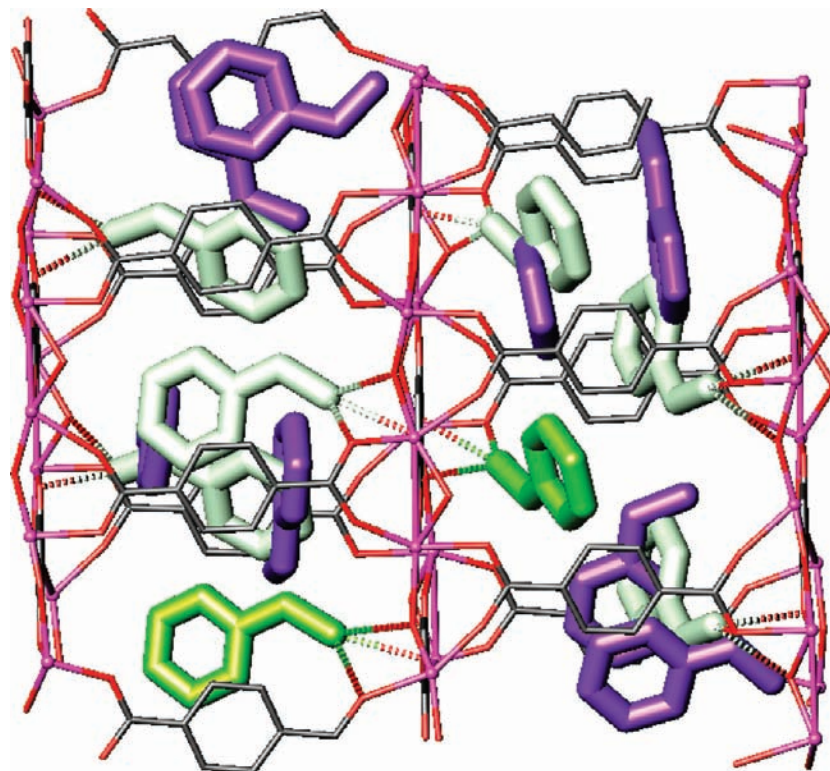


Figure 6. Overlay of the previously determined **EB** positions in MIL-47 (green, gray) on the refined structure of MIL-47 containing **St** (purple). Gray **EB** molecules overlap with **St** pairs (dark gray, carbon; red, oxygen; pink, vanadium; hydrogen atoms have been omitted).

1.8 kJ mol⁻¹ (Table 2; also see Supporting Information).³² Moreover, there is only a small difference between the respective enthalpies obtained from low-pressure vapor-phase experiments (Table 2). Although the adsorption enthalpy is slightly more negative for **EB**, the overall free energy of adsorption, as reflected in K_i , must clearly be more negative for **St** than for **EB**. Thus, the preference of MIL-47 for **St** over **EB** must be based on an entropy effect. To understand the differences in adsorption entropy, siting of the molecules in a saturated MIL-47 framework was studied.

Rietveld refinement was performed on XRD patterns recorded for **St**-saturated MIL-47 (see Supporting Information). The symmetry of MIL-47 is severely affected by the presence of **St** guest molecules, and the structure could only adequately be described by tripling the unit cell in the channel direction with a simultaneous lowering of the space group symmetry from $Pnma$ to $Pn2_1a$. Like xylenes, **St** is packed pairwise in the MIL-47 pores, but as the vinyl substituent is significantly larger than, e.g., the methyl substituent of xylenes, a stacking that is commensurate with the dimensions of the original unit cell cannot be achieved. This causes the observed tripling in the a -direction (Figure 5a). Eight **St** molecules can be hosted as four pairs per tripled unit cell. In each pair, the **St** molecules are approximately parallel with the pore walls, but their aromatic rings do not approach the terephthalate linkers. Instead, the two guest molecules' six-rings are almost aligned, and this allows for π - π interactions. One of the vinyl substituents points toward the framework oxygen atoms of a terephthalate linker and an oxygen atom bridging two vanadium centers, while the other points along the channel direction, i.e., the a -direction. The

behavior of **EB** in MIL-47 has already been described elsewhere (Figure 5b).¹⁵ In contrast with **St**, **EB** does not assume a pairwise packing. Instead, the methyl protons of the conformationally flexible ethyl group of **EB** interact with the oxygen atoms in the pore wall, resulting in only one molecule per single unit cell (see Supporting Information).

With the unique organization of **St** in the pores and the large distance between the **St** pairs, pore space is left available between two consecutive pairs to accommodate additional molecules like **EB**. A theoretical overlay of the known positions of **EB** on the refined structure of **St** in MIL-47 confirms this postulation (Figure 6). Indeed, only one of the originally four possible adsorption sites of **EB** can be occupied without interference from the **St** pairs in the structure. It would thus be logical to assume that this available position can be occupied by **EB**, even when the structure is already saturated with **St**. It can be assumed that **EB** is preferentially accommodated in this free space, as its more flexible sp³-hybridized carbon atoms allow an out-of-plane rotation of the ethyl group to interact with the vanadate octahedra. This results in 10 molecules of C₈ aromatics per 1 tripled unit cell, of which 8 are **St** and 2 are **EB**. This predicts exactly what is found in the competitive adsorption experiments (Figure 1a). Out of a total of 26 wt % of C₈-aromatics being adsorbed at saturation level, ca. 20 wt % consists of **St** (ca. 80%) and the rest is **EB**. The maximal loading of MIL-47 with **EB** and **St** (10 molecules per tripled unit cell) can be compared with the previously reported 12 molecules of *p*-xylene (**pX**) per three unit cells of the same MIL-47 host.¹⁵ This would mean that the uptake of **pX** as a single compound is 1.2 times higher than the sum of the uptake capacities of **St** and **EB** as a mixture, which is in fair agreement with the experimental ratio of 1.3 calculated from 35 wt % **pX** vs 26 wt % **St** + **EB**.¹⁵

(31) Möckel, H.; Dreyer, U. *Chromatographia* **1993**, *37*, 179.

(32) Zhang, Y.; McGuffin, V. *J. Liquid Chromatogr. Relat. Technol.* **2007**, *30*, 1551.

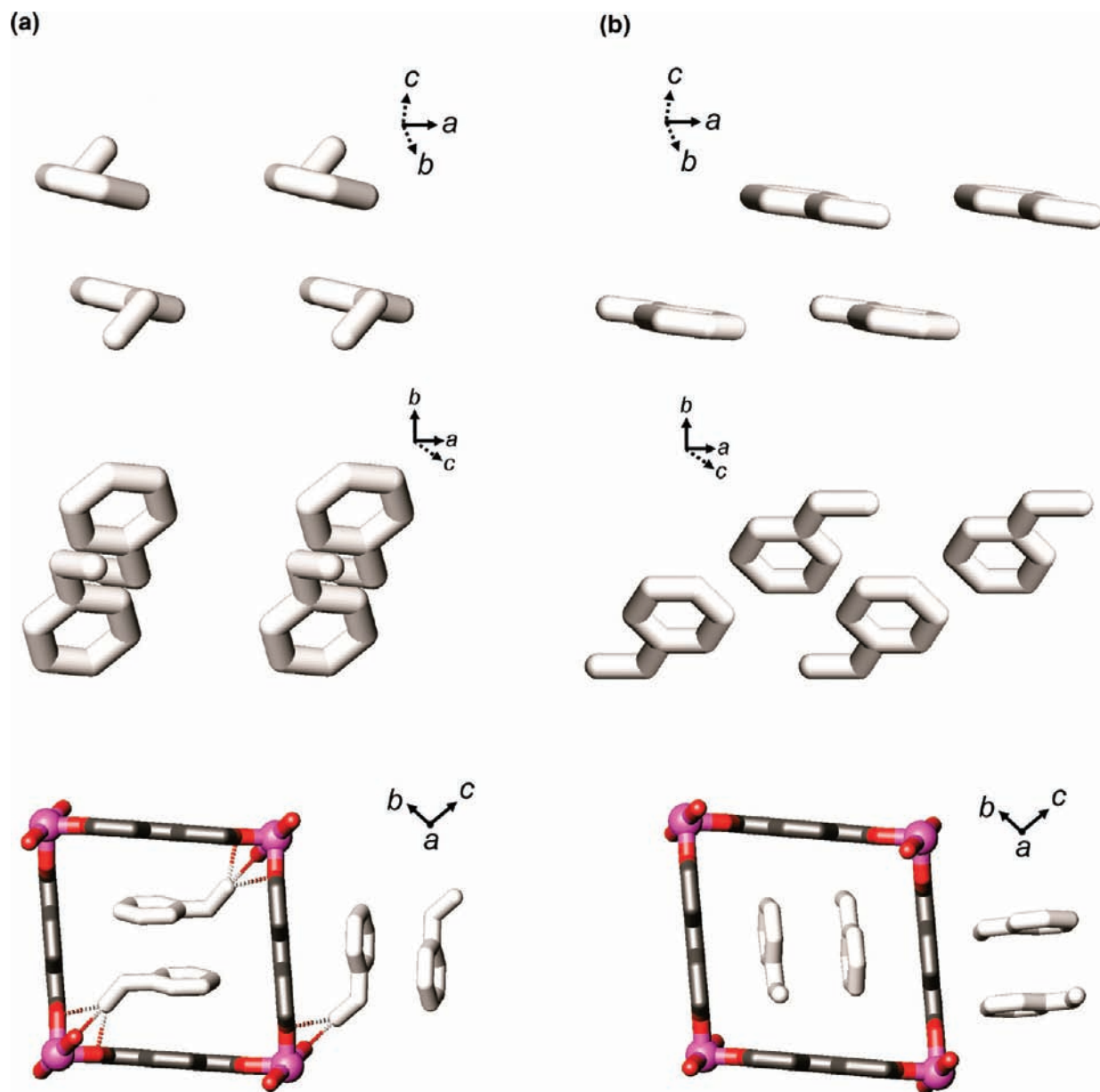


Figure 7. Structure refinements of MIL-53 crystals loaded with (a) **EB** and (b) **St** (gray, carbon; red, oxygen; purple, aluminum; hydrogen atoms have been omitted for clarity).

As four times more **St** than **EB** is adsorbed on MIL-47, it would be logical to assume that the separation factor at high pore loadings would remain constant at 4. This is in good agreement with the results in Figure 1a: the separation factor tends to remain constant at about 3.6 throughout the concentration profile. So, in a tripled unit cell, **EB** molecules can occupy only two of their original 12 positions, while **St** molecules can be accommodated on all of their original 8 positions. This implies a much larger number of possible adsorbate arrangements for **St**, and hence a higher entropy than for **EB**. **EB** thus loses more freedom in the transition from the surrounding liquid to the adsorbed state in the pores, while the adsorption enthalpy is similar for both components. This clearly underpins the idea that entropic effects play a key role in the selectivity mechanism. This mechanism implies that **St** cannot compete for every adsorption site on which **EB** is adsorbed. Therefore, we can now rationalize the fact that the roll-up in Figure 2a is not very pronounced, compared to that observed, e.g., for the separation

Table 3. Lattice Parameters of MIL-47 Crystals Loaded with **EB**¹⁵ and **St**^a

compound	space group	<i>a</i> (Å)	<i>b</i> (Å)	<i>c</i> (Å)
EB ¹⁵	<i>Pnma</i>	6.81	16.41	13.57
St	<i>Pn2₁a</i>	3 × 6.8188(11)	15.6609(19)	14.4447(16)

^a Estimated standard deviation of the last reported digits in parentheses.

of *pX* from *mX* in MIL-47 or *oX* from *mX* on MIL-53.^{15,27} **St** is unable to displace all of the **EB** out of the pores. Furthermore, this mechanism explains why the uptake of **EB** reaches much higher values in single-compound adsorption experiments compared to competitive experiments (Figure 1a, Table 1). As **St** is packed with equal efficiency in the pores in both types of experiments to reach a maximal loading, only a limited amount of pore space remains available to accommodate co-adsorbing **EB** molecules, which is consistent with the guest molecule positions.

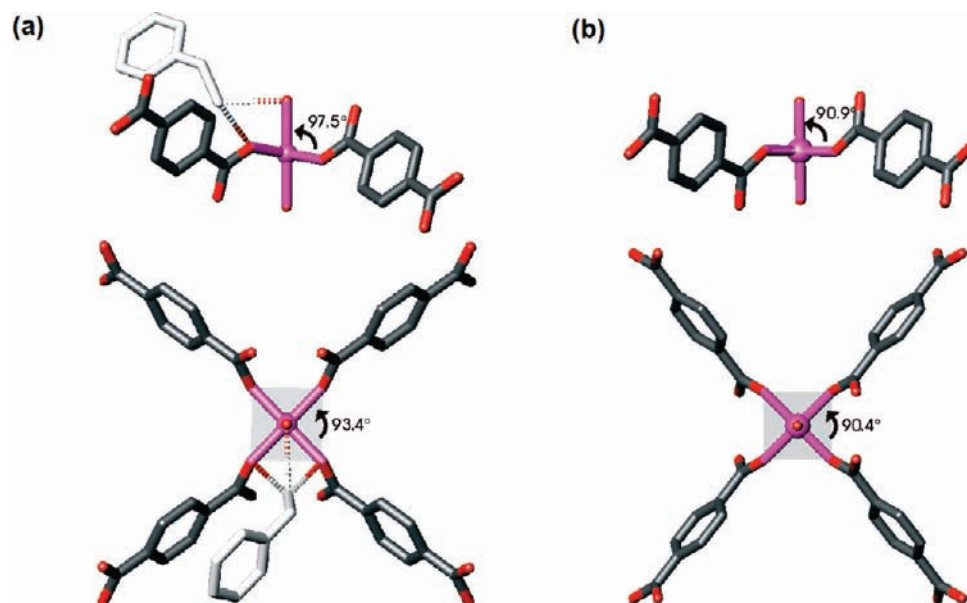


Figure 8. Distortion of the angles of an Al octahedron of MIL-53 caused by (a) **EB** and (b) **St** (gray, carbon; red, oxygen; purple, aluminum; hydrogen atoms have been omitted for clarity; estimated standard deviations of the depicted angles are below $\pm 0.1^\circ$).

Table 4. Sample Composition, Space Group, Lattice Constants, Angles, and Cell Volume of MIL-53 Samples Loaded with **St** and **EB**^a

	MIL-53 ht St	MIL-53 ht EB
phase content (%)	95.95	96.69
<i>a</i> (Å)	6.6424(4)	6.6387(6)
<i>b</i> (Å)	16.0436(11)	15.7610(14)
<i>c</i> (Å)	13.8471(10)	14.1961(14)
α (deg)	90	90
β (deg)	90	90
γ (deg)	90	90
V_{cell} (Å ³)	1475.64(16)	1485.37(22)
symmetry	orthorhombic	orthorhombic
space group	<i>Imma</i>	<i>Imma</i>

^a Estimated standard deviation of last reported digits in parentheses.

In the case of MIL-53, the adsorption mechanism seems to be different. In Figure 4b, **St** and **EB** are baseline-separated at room temperature, resulting in a separation factor of 3.9. This value is similar to those obtained on [Cu₃(BTC)₂].²⁰ However, in contrast with MIL-47, the separation factor decreases with increasing temperature, and from 55 °C on, the peaks of **St** and **EB** start to overlap. A clear dependence of the separation factor on temperature indicates that the adsorption enthalpies of **St** and **EB** must differ significantly (see Supporting Information).³⁰ **EB** has an apparent adsorption enthalpy of -13.1 ± 1.4 kJ mol⁻¹, while the adsorption enthalpy of **St** is much more negative, at -24.2 ± 1.2 kJ mol⁻¹ (Table 2).³¹ This difference in enthalpy corresponds well with the difference in low-coverage adsorption enthalpy obtained from low-pressure vapor-phase experiments in the absence of solvent, i.e., approximately 10.2 kJ mol⁻¹ (-48.9 ± 0.5 kJ mol⁻¹ for **EB** vs -59.1 ± 0.7 kJ mol⁻¹ for **St**) (Table 2).

In order to further understand these differences in adsorption enthalpy between **St** and **EB**, both molecules were localized in the MIL-53 host by Rietveld refinements of XRD patterns of samples saturated with either **St** or **EB** (Figure 7). These samples could be refined in their open form (*Pnma*), but in all cases a similar small amount (<5%) of framework was found in the closed mesh structure in space group *Cc*. **St** and **EB** affect the framework differently. In the case of **EB**, an out-of-plane

rotation of the alkyl group of **EB** is observed, similar to that found in MIL-47. The methyl group is turned toward the framework oxygen atoms of the terephthalate linkers and, more pronouncedly, toward the Al-bridging hydroxy group. In contrast with the relatively rigid MIL-47 structure, MIL-53 is a more flexible structure, and the out-of-plane rotation in **EB** causes a dislocation of the hydroxyl group toward the pore center, with a corresponding distortion of the octahedral environment of the Al ions, resulting in O–Al–O angles of $93.4^\circ \pm 0.1^\circ$ and $97.5^\circ \pm 0.1^\circ$ (Figure 8a). In parallel, the obtuse angle of the rhombic channel, as calculated from the ratio of the *b* and *c* unit cell parameters, is decreased to $96^\circ \pm 0.1^\circ$ (Table 4). In the case of **St**, the environment of Al is an almost perfect octahedron, with all O–Al–O angles very close to 90° (Figures 7b and 8b). This could be due to the fact that **St** consists only of sp²-hybridized carbons, so that an out-of-plane rotation of the vinyl group is impossible. For **St**-loaded MIL-53, the rhombic channel angle is $98.4^\circ \pm 0.1^\circ$ (Table 4), meaning that the structure is significantly less deformed in the presence of **St** than in the presence of **EB**. Note that the open, “ht” form of MIL-53 has an obtuse channel angle of 104.92° in the absence of adsorbates.²²

Thus, it seems that the distortion of the flexible MIL-53 framework induced by **EB** is coupled with an energy cost, and this results in a less negative total apparent enthalpy of adsorption for **EB** in comparison with **St**. This eventually leads to the preferential uptake of **St**, as illustrated in Figures 1b, 2b, and 3. This is in good agreement with the differences in enthalpy reported in Table 2. It can be assumed that one adsorbing molecule of **EB** is already causing this distortion; hence, the differences in enthalpy are already present at the low loadings at which the experiments for enthalpy determination were performed.

4. Conclusion

The metal–organic frameworks MIL-47 and MIL-53 both can separate mixtures of **EB** and **St**. Furthermore, MIL-53 is also capable of purifying an **EB/St** feed by first selectively removing *o*X and toluene impurities. This has been demonstrated

using a combination of batch and column experiments. Both frameworks display similar uptake capacities and separation factors. However, despite the fact that both hosts are structural analogues, the adsorption mechanisms are quite different. On MIL-47, which displays a unique packing of **St**, the co-adsorption of **EB** causes a **St** preference which is based on differences in entropy, while on MIL-53, enthalpic effects play a key role. For **EB** in both cases, an out-of-plane rotation of the ethyl group and interaction with framework oxygen atoms is observed. In the more flexible structure of MIL-53, this results in a significant distortion of the framework, explaining the preference for **St**. Such differences, like these in flexibility, create versatile materials in which many adsorption mechanisms can be found. This makes MOFs one of the most promising

classes of materials to perform both separation and purification of organic process streams.

Acknowledgment. This work has been performed in the frame of the IAP 6/27 Functional Supramolecular Systems of the Belgian Federal Government. L.A. thanks FWO-Vlaanderen (Research Foundation Flanders) for a postdoctoral fellowship. We are grateful to K.U. Leuven for support under the Methusalem grant CASAS.

Supporting Information Available: Details on the calculation of the apparent adsorption enthalpies and the zero coverage adsorption enthalpies as well as details on the crystal structure refinements. This material is available free of charge via the Internet at <http://pubs.acs.org>.

JA106142X